HHS Public Access

Author manuscript

Mol Carcinog. Author manuscript; available in PMC 2020 June 01.

Published in final edited form as:

Mol Carcinog. 2019 June ; 58(6): 996–1007. doi:10.1002/mc.22988.

AKT-dependent sugar addiction by benzyl isothiocyanate in breast cancer cells

Ruchi Roy[1], **Eun-Ryeong Hahm**[1], **Alexander G. White**[2], **Carolyn J. Anderson**[1,3,4,5,6], and **Shivendra V. Singh**[1,6,*]

[1]Department of Pharmacology & Chemical Biology, University of Pittsburgh School of Medicine, Pittsburgh, Pennsylvania 15213, USA.

[2]Department of Microbiology and Molecular genetics, University of Pittsburgh School of Medicine, Pittsburgh, Pennsylvania 15213, USA.

[3]Department of Medicine, University of Pittsburgh School of Medicine, Pittsburgh, Pennsylvania 15213, USA.

[4]Department of Radiology, University of Pittsburgh School of Medicine, Pittsburgh, Pennsylvania 15213, USA.

[5]Department of Bioengineering, University of Pittsburgh School of Medicine, Pittsburgh, Pennsylvania 15213, USA.

[6]UPMC Hillman Cancer Center, University of Pittsburgh School of Medicine, Pittsburgh, Pennsylvania 15213, USA.

Abstract

The overall promise of breast cancer chemoprevention is exemplified by clinical success of selective estrogen receptor modulators and aromatase inhibitors. Despite clinical efficacy, these interventions have limitations, including rare but serious side effects and lack of activity against estrogen receptor-negative breast cancers. We have shown previously that dietary administration of benzyl isothiocyanate (BITC), which occurs naturally as a thioglucoside conjugate in edible cruciferous vegetables, inhibits development of estrogen receptor-negative breast cancer in mouse mammary tumor virus-*neu* (MMTV-*neu*) transgenic mice. This study demonstrates AKT-mediated sugar addiction in breast cancer chemoprevention by BITC. BITC-treated MMTV-*neu* mice exhibited increased 2-deoxy-2-(fluorine-18)-fluoro-D-glucose (^{18}F-FDG) uptake in mammary tumors *in vivo* in comparison with mice fed basal diet. Cellular studies using MDAMB-231 and SUM159 human breast cancer cell lines revealed BITC-mediated induction and punctate localization of glucose transporter GLUT-1, which was accompanied by an increase in intracellular pyruvate levels. BITC treatment resulted in increased S^{473} phosphorylation (activation) of AKT in cells *in vitro* as well as in mammary tumors of MMTV-*neu* mice *in vivo*. Increased glucose uptake, punctate pattern of GLUT-1 localization, and intracellular pyruvate levels resulting from BITC exposure were significantly attenuated in the presence of a

*To whom correspondence should be addressed. Tel: +1 412 623 3263; Fax: +1 412 623 7828; singhs@upmc.edu.

CONFLICT OF INTEREST

The authors declare that no conflict of interest exists.

pharmacological inhibitor of AKT (MK-2206). Inhibition of AKT augmented BITC-mediated inhibition of cell migration and colony formation. BITC-induced apoptotic cell death was also increased by pharmacological inhibition of AKT. These results indicate increased glucose uptake/metabolism by BITC treatment in breast cancer cells suggesting that breast cancer chemoprevention by BITC may be augmented by pharmacological inhibition of AKT.

Keywords

benzyl isothiocyanate; AKT; breast cancer; chemoprevention

1 INTRODUCTION

The epidemiological association of breast cancer risk reduction with increased dietary intake of certain edible plants like cruciferous vegetables is fairly-compelling. For example, it was concluded recently that increased dietary intake of cruciferous and yellow/orange vegetables (>5.5 servings/day *versus* ≤2.5 servings/day) was inversely associated with the risk of breast cancer (P_{trend} = 0.005) among 182,145 women in the Nurses' Health Study.[1] In a hospital-based case-control study of 1491 patients with breast cancer and 1482 controls, the overall risk of breast cancer was also found to be inversely associated with cruciferous vegetable intake.[2] Isothiocyanates (R-N=C=S) are believed to be the predominant bioactive phytochemicals with anti-cancer activity in edible cruciferous vegetables.[3] The isothiocyanates are generated upon myrosinase-mediated metabolism of corresponding glucosinolate precursors.[3] Chemical diversity of isothiocyanates in different plants is represented by various side chain modifications, including aliphatic (straight- or branched-chain), aromatic, aliphatic straight and branched-chain alcohols, alkyl-thio-alkyl, olefins and so forth.[4] Benzyl isothiocyanate (BITC), an aromatic isothiocyanate, appears promising for chemoprevention of breast cancer based on data from numerous preclinical studies.[5] For example, BITC administration was shown to inhibit the occurrence of 7,12-dimethylbenz(a)anthracene-induced breast cancer in female Sprague-Dawley rats.[6] Dietary feeding of BITC markedly suppressed the incidence and/or burden of mammary hyperplasia and carcinoma in female mouse mammary tumor virus-*neu* (MMTV-*neu*) mice without any side effects.[7] Interestingly, BITC administration through diet (3 μmol BITC/g diet for 29 weeks) also resulted in a marked decrease in fraction of breast cancer stem-like cells in the mammary tumors of MMTV-*neu* mice.[8] The *in vivo* therapeutic efficacy of BITC for inhibition of breast cancer growth has been demonstrated using human (MDA-MB-231) and murine (4T1) xenograft models in immunocompromised (female nude mice) and immunocompetent mice (female BALB/c mice), respectively.[9–10] The *in vivo* growth of subcutaneously implanted MDAMB-231 cells was inhibited significantly upon intra-peritoneal administration of BITC.[9] Similarly, oral administration of BITC (10 mg/kg body weight/day) resulted in a significant inhibition of solid tumor growth of 4T1 cells orthotopically injected into the inguinal mammary fat pads of female syngeneic BALB/c mice.[10] We have also shown recently that BITC is a potent inhibitor of breast cancer-induced osteoclastogenesis *in vitro* and *in vivo*.[11] Specifically, BITC treatment decreased breast cancer cell-induced differentiation of osteoclast precursor cells *in vitro*.[11] Moreover, oral administration of 10 mg BITC/kg body weight (5 times/week) inhibited MDA-MB-231-

induced skeletal metastasis multiplicity by about 81% when compared with control (P = 0.04).[11]

Identification of the molecular regulators of chemopreventive effect of BITC in breast cancer is desirable for various reasons. First, the mechanistic insight into breast cancer chemoprevention by BITC could lead to identification of pharmacodynamic biomarkers potentially useful in future clinical trials. Second, mechanistic studies could facilitate conceptualization of novel BITC-based combination regimens. We have shown previously that BITC inhibits complex III of the mitochondrial respiratory chain and possibly suppresses oxidative phosphorylation.[12] However, the effect of BITC on glucose uptake and utilization (glycolysis) is yet to be studied. Increased glycolysis is now considered a hallmark of cancers including breast cancer,[13] a phenomenon more commonly known as Warburg effect.[14] The present study was undertaken to determine the effect of BITC treatment on glucose uptake and metabolism using human breast cancer cell lines (MDA-MB-231 and SUM159) and MMTV-*neu* mice as models.

2 MATERIALS AND METHODS

2.1 Ethics statement

The MMTV-*neu* mice were used to determine the effect of BITC administration on glucose uptake in mammary tumors. Use of mice was approved by the Institutional Animal Care and Use Committee.

2.2 Reagents and cell lines

BITC (purity-about 98%) was purchased from LKT Laboratories (St. Paul, MN). Stock solution of BITC was prepared in dimethyl sulfoxide (DMSO) and an equal volume of DMSO (final concentration-0.05%) was added to the controls. Reagents for cell culture [fetal bovine serum (FBS) and antibiotics] as well as Alexa Fluor 488-conjugated anti-rabbit antibody were purchased from Invitrogen (part of ThermoFisher Scientific, Waltham, MA). An antibody against glucose transporter 1 (GLUT-1) was purchased from Abcam (Cambridge, MA). Antibodies specific for detection of phosphorylated p-Ser^{473}-AKT, p-Thr^{308}-AKT, lactate dehydrogenase A (LDHA), pyruvate dehydrogenase (PDH), hexokinase II (HK II), and AKT kinase assay kit were purchased from Cell Signaling Technology (Beverly, MA). Anti-pyruvate kinase M2 (PK-M2) antibody was purchased from Abgent (San Diego, CA). Anti-glyceraldehyde-3-phosphate dehydrogenase (GAPDH) antibody was from GeneTex (Irvine, CA). Other reagents including 4’,6-diamidino-2-phenylindole (DAPI) and propidium iodide (PI) were from Sigma-Aldrich (St. Louis, MO). The AKT inhibitor (AKTi; MK-2206) {(8-(4-(1-aminocyclobutyl)phenyl)-9-phenyl-[1,2,4]triazolo[3,4-f][1,6]naphthyridin-3(2H)-one} was purchased from Selleckchem (Houston, TX). Apoptosis detection kit was purchased from BD Biosciences (San Diego, CA). Kits for measurement of glucose, lactate, pyruvate, and acetyl CoA were purchased from BioVision (Milpitas, California).

MDA-MB-231 and SUM159 cell lines were purchased from the American Type Culture Collection (Manassas, VA) and Asterand Bioscience (Detroit, MI), respectively. The cells

were cultured as recommended by the suppliers. Both cell lines were last authenticated in January of 2015 and March of 2018. The cell lines were found to be of human origin and authentic.

2.3 Two-dimensional gel electrophoresis and mass spectrometry

Tumor tissues from three different mice of each group were used to determine treatment-related protein alterations by two-dimensional gel electrophoresis followed by matrix-assisted laser desorption ionization-time of flight/time of flight (MALDI-TOF/TOF) (Applied Biomics, Hayward, CA) as described by us previously.[15]

2.4 2-Deoxy-2-(fluorine-18)-fluoro-D-glucose (^{18}F-FDG)-positron emission tomography/computed tomography (PET/CT)

Six-week old female transgenic MMTV-*neu* mice were purchased from Jackson Laboratories and acclimated for 2 weeks prior to start of the experiment. The mice were either placed on a basal AIN-76A diet (control group) or the same diet supplemented with 3 mmol BITC/kg diet. The diet was replaced every 3–4 days at the time of cage change. Mice were sacrificed at 33 weeks of age. PET/CT imaging was performed using an Inveon Preclinical Scanner (Siemens Preclinical; Knoxville, TN). Mice were injected with 100 ± 10 μCi ^{18}F-FDG (IBA Worldwide, Dulles, VA) in 1 × phosphate-buffered saline (PBS) *via* the tail vein. Following a one-hour incubation period, mice were anesthetized with 5% v/v isoflurane with an O_2 flow rate of 2 L/min for induction and 2–2.5% v/v with an O_2 flow rate of 2 L/min for anesthetic maintenance during imaging. PET acquisition parameters: 300–600 second acquisition, 2DFBP reconstruction algorithm was used for data analysis, OSEM3D/MAP algorithm was used for final image files. CT acquisition was used as an attenuation map for PET reconstruction and for anatomical marking purposes. CT acquisition parameters: 150 second total imaging time in one-degree intervals over a 240-degree scanning path (Multi-bed acquisition, binning factor 4, X-ray source voltage=80 mV; current = 300 μA). All image acquisition and processing were performed using Inveon Acquisition Workplace and image analysis was performed on Inveon Research Workplace (Siemens Preclinical; Knoxville, TN). Volume-of-interest analysis was performed and Standardized Uptake Values by body weight and *%* ID/g value was obtained.

2.5 Determination of glucose uptake in breast cancer cell lines

MDA-MB-231 or SUM159 cells (1×10^5 cells/well) were seeded in 12-well plates in RPMI 1640 media containing 2.5 mM glucose and 2% FBS. After completion of BITC +/− AKTi treatment, 2-deoxyglucose was added to each well, and the plates were incubated at 37°C for 20 min. Further sample processing was performed according to the instructions provided by the manufacturer of the kit. The absorbance was measured at 405 nm by using a spectrophotometer.

2.6 Immunofluorescence microscopy for GLUT-1 expression

MDA-MB-231 or SUM159 cells (5×10^4 cells/well) were seeded on cover slips in 24-well plates, and treated with DMSO (control) or 2.5 μM BITC for 24 h followed by fixation and permeabilization with CytoFix/CytoPerm buffer for 20 min at room temperature. The cells

were treated with blocking buffer containing 0.5% bovine serum albumin (BSA) and 0.15 % glycine in PBS for 1 h at room temperature. Cells were then incubated with anti-GLUT-1 (1:1000 dilution) antibody in blocking buffer overnight at 4°C. Cells were stained with Alexa Fluor 488-conjugated secondary antibody (1:2000 dilution) for 2 h at room temperature. The cells were stained with DAPI prior to mounting. Immunofluorescence was examined under a Leica DC300F fluorescence microscope. Experiment was done twice with consistent results and representative data from one such experiment is shown as mean ± SD (n = 3)

2.7 Western blotting

MDA-MB-231 or SUM159 cells were exposed to different concentrations of BITC for 6 and 12 h. In some experiments, MDA-MB-231 or SUM159 cells were treated with DMSO or 2.5 μM of BITC in the absence or presence of 200 nM AKTi for 24 h. The cells were washed with PBS and then lysates were processed for western blotting as described by us previously.[16] Immunoreactive bands were visualized by enhanced chemiluminescence method.

2.8 Determination of lactate, pyruvate, and acetyl CoA levels

MDA-MB-231 or SUM159 cells (5×10^5 cells) were seeded in 6 cm dishes. After 24 h of BITC or DMSO treatment, supernatant was removed, followed by addition of 2 mL phenol red and FBS free media for 45 min. Released lactate was measured according to the manufacturers' protocol. The absorbance was measured at 570 nm. Intracellular pyruvate level was measured according to the manufacturers' protocol. Briefly, MDA-MB-231 or SUM159 cells (5×10^5 cells) were seeded in 6 cm dishes. After completion of BITC +/− AKTi treatment, pyruvate was measured at 570 nm. Acetyl CoA level was determined as recommended by the supplier of the kit. Fluorescence was measured at an excitation of 535 nm and emission of 587 nm.

2.9 Analysis of RNA-seq expression profile in The Cancer Genome Atlas (TCGA)

Association of *AKT* expression with that of key glycolysis genes (*HKII, PKM2*, and *LDHA*) was determined by RNA-Seq expression profiles in breast cancer TCGA data set using University of California Santa Cruz Xena Browser (http://xena.ucsc.edu/public-hubs/).

2.10 AKT kinase assay

Desired cells were exposed to 2.5 and 5 μM BITC for 6 and 12 h and then the lysates were prepared according to the manufacturers' protocol. AKT kinase assay was performed as suggested by the manufacturer of the kit.

2.11 Immunohistochemistry

Mammary gland sections from control and BITC-treated MMTV-*neu* mice were deparaffinized and rehydrated. The sections were then quenched with 3% hydrogen peroxide followed by treatment for 60 min at room temperature with the desired primary antibody. The sections were incubated for 30 min at room temperature with Envision+ Dual Link (Dako-Agilent Technologies). A characteristic brown color was developed with 3,3'-diaminobenzidine. Stained sections were examined under a Leica DC300F microscope at

200 × magnifications. At least three non-overlapping representative images were captured from each section and analyzed using Aperio ImageScope v9.1 software (Aperio, Vista, CA) for GLUT-1 expression using membrane intensity algorithm and for p-Ser^{473}-AKT level using positive pixel algorithm. Results for p-Ser^{473}-AKT and GLUT-1 are expressed as H-score.[16]

2.12 Cell migration

MDA-MB-231 (2×10^5) or SUM159 cells (1×10^5) were suspended in serum-free medium and placed in triplicates on the upper compartment of Boyden Chamber containing 8 μm filter for migration assay. After 24 h of incubation with BITC or BITC in combination with AKTi, nonmotile cells were removed from the upper surface of the filter. The motile cells on the bottom face of the filter were fixed with methanol and stained with hematoxylin and eosin for 3–5 min. At least three regions were examined on each sample (magnification = 200 ×).

2.13 Clonogenic assay

MDA-MB-231 or SUM159 cells were seeded in 6-well plates in triplicates at a density of 500 cells/well. After overnight incubation, cells were treated with BITC or BITC in combination with AKTi, and the media was replaced with fresh medium containing treatment every 3rd day. After 10 days, colonies were stained with crystal violet (0.1% in 20% methanol).

2.14 Measurement of apoptosis

Apoptosis induction in cells following treatment with BITC +/− AKTi (MK-2206, AKT inhibitor) was determined by AnnexinV/PI binding assay as described by us previously.[17]

2.15 Statistical analysis

Statistical significance of difference in measured variables was determined by one-way analysis of variance (ANOVA) followed by Dunnett's test or Newman-Keuls multiple comparisons test. Statistical significance of differences for ^{18}F-FDG uptake, GLUT-1 puncta per cell, and H-score between control and BITC treated groups was determined by Student t-test. Difference was considered significant at $P < 0.05$. All statistical tests were done using GraphPad Prism version6.07 software.

3 RESULTS

3.1 BITC treatment increased ^{18}F-FDG uptake in mammary tumors of *MMTV-neu* mice

Unbiased proteomic analysis of mammary tumors from control and BITC-treated MMTV-*neu* mice revealed changes in levels of proteins related to glycolysis, including GAPDH, PKM1/2, phosphoglycerate kinase, LDH, etc. (data not shown). These observations prompted us to determine whether BITC treatment alters glucose uptake. Figure 1A shows PET/CT images for a representative mouse of the control group and a mouse of the BITC treatment group. In two separate experiments, MMTV-*neu* mice placed on BITC-supplemented diet exhibited a significant increase in ^{18}F-FDG uptake by the spontaneously

developing mammary tumor as compared to mice fed basal diet (representative data from one such experiment is shown in Figure 1B). Consistent with PET/CT data, exposure of MDA-MB-231 cells to BITC resulted in an increase in glucose uptake that was statistically significant at 2.5 μM BITC concentration, which is pharmacologically relevant,[18] in comparison with DMSO-treated controls (Figure 1C). These results indicated that BITC treatment caused an increase in ^{18}F-FDG and glucose uptake by breast cancer cells *in vivo* and *in vitro*.

3.2 BITC treatment increased GLUT-1 expression in breast cancer cells

GLUT-1 plays an important role in the transport of glucose in cancer cells.[19–20] We therefore raised the question of whether BITC treatment increased GLUT-1 expression to facilitate glucose uptake by breast cancer cells. As can be seen in Figure 2A, BITC-treated MDA-MB-231 and SUM159 cells exhibited a marked increase and punctate localization of GLUT-1 when compared to corresponding vehicle-treated control cells. The average number of GLUT-1 puncta/cell was significantly higher in BITC-treated cells than in control cells (Figure 2B). Immunoblotting confirmed induction of GLUT-1 protein upon treatment with BITC in comparison with control cells (Figure 2C). These results indicated that BITC-mediated increase in glucose uptake was likely due to increased expression of GLUT-1 protein.

3.3 BITC-mediated changes in glucose metabolism-related proteins

Next, we determined the effect of BITC treatment on expression of key cancer-relevant glucose metabolizing enzyme proteins, including HK II (which catalyzes the phosphorylation of glucose), PK-M2 (which converts phosphoenolpyruvate to pyruvate), LDHA (which catalyzes conversion of pyruvate to lactate), and PDH (which contributes to transformation of pyruvate to acetyl CoA), and the results are shown in Figure 3A. Most of these proteins are overexpressed in breast cancer and are considered prognostic biomarkers.[21–23] The protein levels of HK II, PK-M2, and PDH were increased upon treatment of MDA-MB-231 and SUM159 cells with BITC when compared to control especially at the 2.5 μM concentration (Figure 3A). On the other hand, the protein level of LDHA was decreased in BITC-treated cells in comparison with vehicle-treated control cells (Figure 3A). Analyses of the glucose metabolism intermediates revealed an increase in levels of pyruvate and acetyl CoA but a decrease in lactate levels upon BITC treatment (Figure 3B–D). These results indicated that BITC treatment promoted conversion of glucose to pyruvate and acetyl CoA.

3.4 BITC treatment caused activation of AKT in breast cancer cells

AKT activation has been suggested to regulate glucose uptake by cancer cells.[24] Analysis of the RNA-Seq data in the breast cancer TCGA (n = 1097 primary tumors) also revealed a significant positive association between expression of *AKT1* and *HKII* (Pearson's r = 0.1507; $P < 0.0001$) and *PK-M2* (Pearson's r = 0.2689; $P < 0.0001$) but not *LDHA* (Pearson's r = −0.0298; P = 0.3240). We next proceeded to determine the effect of BITC on phosphorylation (activation) of AKT. BITC-treated cells exhibited increased phosphorylation of AKT at Thr^{308} and Ser^{473} sites especially at 12 h time point (Figure 4A). AKT kinase assay also indicated BITC-mediated activation of AKT (Figure 4B). Therefore, to further elucidate the role of AKT in promotion of aerobic glycolysis, the effect of its

pharmacological inhibition on glucose consumption and pyruvate production was determined. As can be seen in Figure 4C, BITC-mediated AKT activation was abolished in the presence of AKTi (MK-2206). Increased glucose uptake (Figure 4D), GLUT-1 puncta/cell (Figure 5A), and intracellular pyruvate level (Figure 5B) resulting from BITC treatment was also significantly attenuated by MK-2206 treatment. Mammary tumor sections from control and BITC-treated MMTV-*neu* mice immunostained using anti-Ser^{473} phosphorylated AKT and anti-GLUT-1 antibodies and the results are shown in Figure 5C. Levels of both Ser^{473} phosphorylated AKT and GLUT-1 were higher in mammary tumors of BITC-treated mice (n = 4) in relation to control (n = 3), and the difference was statistically significant for GLUT-1 even with a small sample size (Figure 5D). These results indicated BITC-mediated increase in glucose uptake and conversion to pyruvate was dependent on AKT activation.

3.5 AKT activation negated BITC-mediated inhibition of migration and colony formation

Figure 6A shows migration potential of MDA-MB-231 and SUM159 cells in the presence of BITC and/or AKTi. Migration of both cell lines was inhibited significantly in the presence of BITC or AKTi alone (Figure 6B). However, the BITC-mediated suppression of MDA-MB-231 or SUM159 cell migration was augmented in the presence of AKTi (Figure 6B). Similarly, clonogenic assays revealed amplification of MDA-MB-231 and SUM159 cell growth inhibition in the presence of both BITC and AKTi (Figures 6C and 6D). In agreement with these results, apoptotic cell death resulting from BITC treatment was increased in the presence of AKTi (Figure 6E). These results indicated that AKT activation negated BITC-mediated inhibition of MDA-MB-231 and SUM159 cell migration and growth.

4. DISCUSSION

The glucose uptake by mammalian cells is facilitated by GLUT family members.[19] Of the 14 isoforms, GLUT-1 is the primary mediator of glucose uptake by mammary cells.[19] Analysis of tissue microarrays with cores of normal breast tissue, ductal hyperplasia, ductal carcinoma *in situ*, invasive ductal carcinoma, and lymph node metastases revealed membrane expression of GLUT-1 in normal and cancerous tissues.[25] Interestingly, roughly 38% of the invasive ductal carcinoma showed GLUT1 expression that was significantly correlated with higher histologic grade, larger tumor size, loss of estrogen and progesterone receptors as well as triple-negative phenotype.[25] In another study, GLUT-1 expression in breast cancer was associated with high proliferation and total histologic score.[26] Knockdown of GLUT-1 in breast tumor cell lines resulted in decreased glucose transport and consumption and an opposite trend was observed upon its overexpression.[27] The present study reveals that cancer chemopreventive phytochemical BITC increases glucose uptake and utilization by mammary cancer cells *in vitro* as well as *in vivo*. It is reasonable to postulate that breast cancer chemoprevention by BITC may be augmented by inhibition of glucose uptake. This premise is partly supported by the results shown herein where inhibition of glucose uptake by AKTi augments BITC-mediated suppression of cell migration and growth *in vitro*.

Glucose is eventually metabolized to pyruvate that is either converted to lactic acid by LDHA or to acetyl-CoA, and the later intermediate is used in the citric acid cycle for cellular respiration. The results of the present study indicate that BITC-treated breast cancer cells favor conversion of pyruvate to acetyl-CoA. BITC treatment not only increases intracellular level of pyruvate but also induces the expression of pyruvate dehydrogenase that is responsible for conversion of pyruvate to acetyl-CoA. Consistent with these results, intracellular levels of acetyl-CoA increase upon treatment of breast cancer cells with BITC. Because acetyl-CoA is the building of *de novo* lipogenesis, it would be interesting to determine whether BITC treatment increases fatty acid synthesis and/or oxidation.

We found that increased glucose uptake and utilization upon BITC treatment in MDAMB-231 and SUM159 cells is facilitated by AKT activation. In this context, it was shown recently that culturing MCF-7 breast cancer cells in high-glucose conditions promoted AKT phosphorylation and anchorage-independent growth.[28] In the present study, we show that BITC treatment causes activation of AKT and its pharmacological inhibition abolishes glucose uptake and utilization promoted by BITC. Inhibition of AKT also augments anticancer effects of BITC, including suppression of cell migration/growth and apoptosis induction. These results indicate that AKT activation impedes anticancer effects of AKT at least in breast cancer cells.

It is important to point out that in contrast to the results of the present study, BITC treatment was shown to inhibit AKT in other types of cancer cells including non-small cell lung cancer and pancreatic cancer cells.[29–30] However, BITC-mediated inhibition of AKT in these cell lines was observed at 10 and 20 μM concentrations.[29–30] BITC is highly cytotoxic at these high concentrations at least in MDA-MB-231 and MCF-7 cells.[31] Thus, the discrepancy between published results in other cancer types and our data is likely attributable to BITC dose as well as cell line-specific differences.

In summary, the present study reveals that BITC treatment causes activation of AKT kinase leading to increased glucose uptake and utilization *in vitro* and *in vivo*. We demonstrate further that anticancer effects of BITC (inhibition of cell migration and growth, and apoptotic death) are augmented by pharmacological inhibition of AKT.

ACKNOWLEDGEMENT

The authors thank Joseph D. Latoche for assistance with PET/CT, and Kamayani Singh for preparation of the manuscript. This study was supported by the National Cancer Institute grant CA129347 (to SVS). This research used the Animal Facility, the Flow Cytometry Facility, the *In Vivo* Imaging Facility, and the Tissue and Research Pathology Facility supported in part by a grant from the National Cancer Institute (P30 CA047904; Dr. Robert L. Ferris-Principal Investigator).

Abbreviations:

ANOVA	analysis of variance
AKTi	AKT inhibitor MK-2206
BITC	benzyl isothiocyanate

BSA	bovine serum albumin
CT	computed tomography
DAPI	4’,6-diamidino-2-phenylindole
DMSO	dimethyl sulfoxide
FBS	fetal bovine serum
^{18}F-FDG	2-deoxy-2-(fluorine-18)-fluoro-D-glucose
GAPDH	glyceraldehyde-3-phosphate dehydrogenase
GLUT-1	glucose transporter 1
HK II	hexokinase II
LDHA	lactate dehydrogenase A
MALDI-TOF/TOF	matrix-assisted laser desorption ionization-time of flight/ time of flight
MMTV-*neu*	mouse mammary tumor virus-*neu*
PBS	phosphate-buffered saline
PDH	pyruvate dehydrogenase
PET	positron emission tomography
PI	propidium iodide
PK-M2	pyruvate kinase-M2

REFERENCES

1. Farvid MS, Chen WY, Rosner BA, Tamimi RM, Willett WC, Eliassen AH. Fruit and vegetable consumption and breast cancer incidence: Repeated measures over 30 years of follow-up. Int J Cancer. 2018; in press (doi: 10.1002/ijc.31653)
2. Lin T, Zirpoli GR, McCann SE, Moysich KB, Ambrosone CB, Tang L. Trends in cruciferous vegetable consumption and associations with breast cancer risk: A case-control study. Curr Dev Nutr. 2017;1:e000448. [PubMed: 29955715]
3. Conaway CC, Yang YM, Chung FL. Isothiocyanates as cancer chemopreventive agents: their biological activities and metabolism in rodents and humans. Curr DrugMetab. 2002;3:233–255.
4. Fahey JW, Zalcmann AT, Talalay P. The chemical diversity and distribution of glucosinolates and isothiocyanates among plants. Phytochem. 2001;56:5–51.
5. Singh SV, Singh K. Cancer chemoprevention with dietary isothiocyanates mature for clinical translational research. Carcinogenesis. 2012;33:1833–1842. [PubMed: 22739026]
6. Wattenberg LW. Inhibition of carcinogen-induced neoplasia by sodium cyanate, tert-butyl isocyanate, and benzyl isothiocyanate administered subsequent to carcinogen exposure. Cancer Res. 1981;41:2991–2994. [PubMed: 6788365]
7. Warin R, Chambers WH, Potter DM, Singh SV. Prevention of mammary carcinogenesis in MMTV-*neu* mice by cruciferous vegetable constituent benzyl isothiocyanate. Cancer Res. 2009;69:9473–9480. [PubMed: 19934325]

8. Kim SH, Sehrawat A, Singh SV. Dietary chemopreventative benzyl isothiocyanate inhibits breast cancer stem cells *in vitro* and *in vivo*. Cancer PrevRes (Phila). 2013;6:782–790.
9. Warin R, Xiao D, Arlotti JA, Bommareddy A, Singh SV. Inhibition of human breast cancer xenograft growth by cruciferous vegetable constituent benzyl isothiocyanate. Mol Carcinog. 2010;49:500–507. [PubMed: 20422714]
10. Kim EJ, Hong JE, Eom SJ, Lee JY, Park JH. Oral administration of benzyl-isothiocyanate inhibits solid tumor growth and lung metastasis of 4T1 murine mammary carcinoma cells in BALB/c mice. Breast Cancer Res Treat. 2011;130:61–71. [PubMed: 21170677]
11. Pore SK, Hahm ER, Latoche JD, Anderson CJ, Shuai Y, Singh SV. Prevention of breast cancer-induced osteolytic bone resorption by benzyl isothiocyanate. Carcinogenesis. 2018;39:134–145. [PubMed: 29040431]
12. Xiao D, Powolny AA, Singh SV. Benzyl isothiocyanate targets mitochondrial respiratory chain to trigger reactive oxygen species-dependent apoptosis in human breast cancer cells. J Biol Chem. 2008;283:30151–30163. [PubMed: 18768478]
13. Hanahan D, Weinberg RA. Hallmarks of cancer: The next generation. Cell. 2011;144:646–674. [PubMed: 21376230]
14. Warburg O On the origin of cancer cells. Science. 1956;123:309–314. [PubMed: 13298683]
15. Hahm ER, Lee J, Kim SH, et al. Metabolic alterations in mammary cancer prevention by withaferin A in a clinically relevant mouse model. J Natl Cancer Inst. 2013;105:1111–1122. [PubMed: 23821767]
16. Xiao D, Srivastava SK, Lew KL, et al. Allyl isothiocyanate, a constituent of cruciferous vegetables, inhibits proliferation of human prostate cancer cells by causing G2/M arrest and inducing apoptosis. Carcinogenesis. 2003;24:891–897. [PubMed: 12771033]
17. Sakao K, Singh SV. D,L-Sulforaphane-induced apoptosis in human breast cancer cells is regulated by the adapter protein $p66^{Shc}$. J Cell Biochem. 2012;113:599–610. [PubMed: 21956685]
18. Sehrawat A, Singh SV. Molecular mechanisms of cancer chemoprevention with benzyl isothiocyanate In: Inflammation, Oxidative Stress, and Cancer: Dietary Approaches for Cancer Prevention (Kong AN, ed.), CRC Press, Taylor & Francis Group; 2013 pp. 447–462.
19. Zhao FQ. Biology of glucose transport in the mammary gland. J Mammary Gland Biol Neoplasia. 2014;19:3–17. [PubMed: 24221747]
20. Wang J, Ye C, Chen C, et al. Glucose transporter GLUT1 expression and clinical outcome in solid tumors: a systematic review and meta-analysis. Oncotarget. 2017;8:16875–16886. [PubMed: 28187435]
21. Smith TA. Mammalian hexokinases and their abnormal expression in cancer. Br J Biomed Sci. 2000;57:170–178. [PubMed: 10912295]
22. Yang Y, Wu K, Liu Y, Shi L, Tao K, Wang G. Prognostic significance of metabolic enzyme pyruvate kinase M2 in breast cancer: A meta-analysis. Medicine (Baltimore). 2017;96:e8690. [PubMed: 29145305]
23. Huang X, Li X, Xie X, et al. High expressions of LDHA and AMPK as prognostic biomarkers for breast cancer. Breast. 2016;30:39–46. [PubMed: 27598996]
24. Young CD, Anderson SM. Sugar and fat-that's where it's at: metabolic changes in tumors. Breast Cancer Res. 2008;10:1–9.
25. Jang SM, Han H, Jang KS, et al. The glycolytic phenotype is correlated with aggressiveness and poor prognosis in invasive ductal carcinomas. J Breast Cancer. 2012;15: 172–180. [PubMed: 22807934]
26. Younes M, Brown RW, Mody DR, Fernandez L, Laucirica R. GLUT1 expression in human breast carcinoma: correlation with known prognostic markers. Anticancer Res. 1995;15:2895–2898. [PubMed: 8669885]
27. Young CD, Lewis AS, Rudolph MC, et al. Modulation of glucose transporter 1 (GLUT1) expression levels alters mouse mammary tumor cell growth in vitro and in vivo. PLoS One. 2011;6:e23205. [PubMed: 21826239]
28. Matsui C, Takatani-Nakase T, Maeda S, Takahashi K. High-glucose conditions promote anchorage-independent colony growth in human breast cancer MCF-7 cells. Biol Pharm Bull. 2018;41:1379–1383. [PubMed: 30175774]

29. Boreddy SR, Pramanik KC, Srivastava SK. Pancreatic tumor suppression by benzyl isothiocyanate is associated with inhibition of PI3K/AKT/FOXO pathway. Clin Cancer Res. 2011;17:1784–1795. [PubMed: 21350002]

30. Wu X, Zhu Y, Yan H, et al. Isothiocyanates induce oxidative stress and suppress the metastasis potential of human non-small cell lung cancer cells. BMC Cancer. 2010;10:269. [PubMed: 20534110]

31. Xiao D, Vogel V, Singh SV. Benzyl isothiocyanate-induced apoptosis in human breast cancer cells is initiated by reactive oxygen species and regulated by Bax and Bak. Mol Cancer Ther. 2006;5:2931–2945. [PubMed: 17121941]

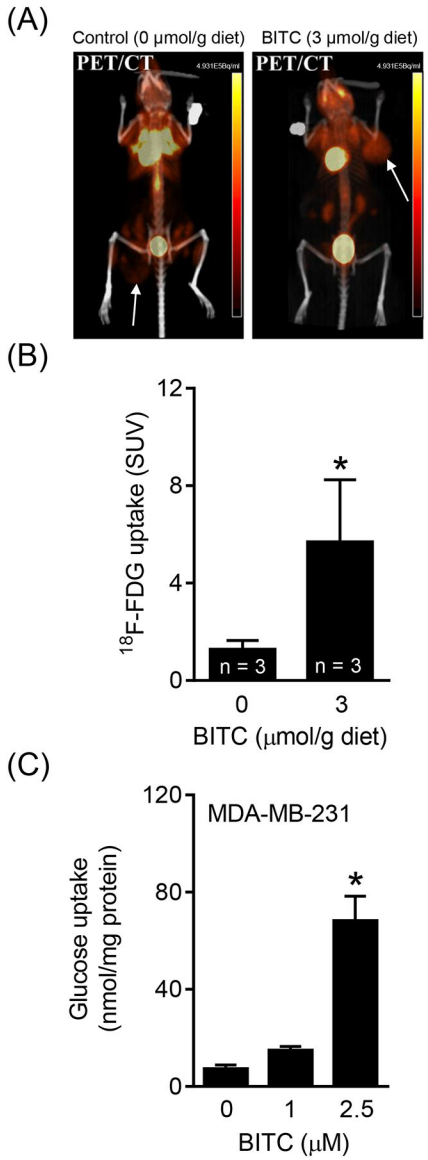

FIGURE 1.

BITC administration increases ^{18}F-FDG uptake in tumors of MMTV-*neu* mice. (A) PET/CT images for a control mouse and a BITC-treated MMTV-*neu* mouse show differential ^{18}F-FDG uptake. Location of tumor is indicated by arrows. (B) Quantification of ^{18}F-FDG uptake in MMTV-*neu* mice of each group. Data are shown as mean ± SD (n = 3). Statistical significance of differences (*, $P < 0.05$) was determined by unpaired Student *t* test. (C) Level of glucose uptake was determined in MDA-MB-231 human breast cancer cells after 24 h treatment with BITC (1 and 2.5 μM). Experiments were done at least twice with consistent results and representative data are shown as mean ± SD (n = 4). Statistical significance of differences (*, $P < 0.05$) was determined by One-way ANOVA followed by Dunnett's test.

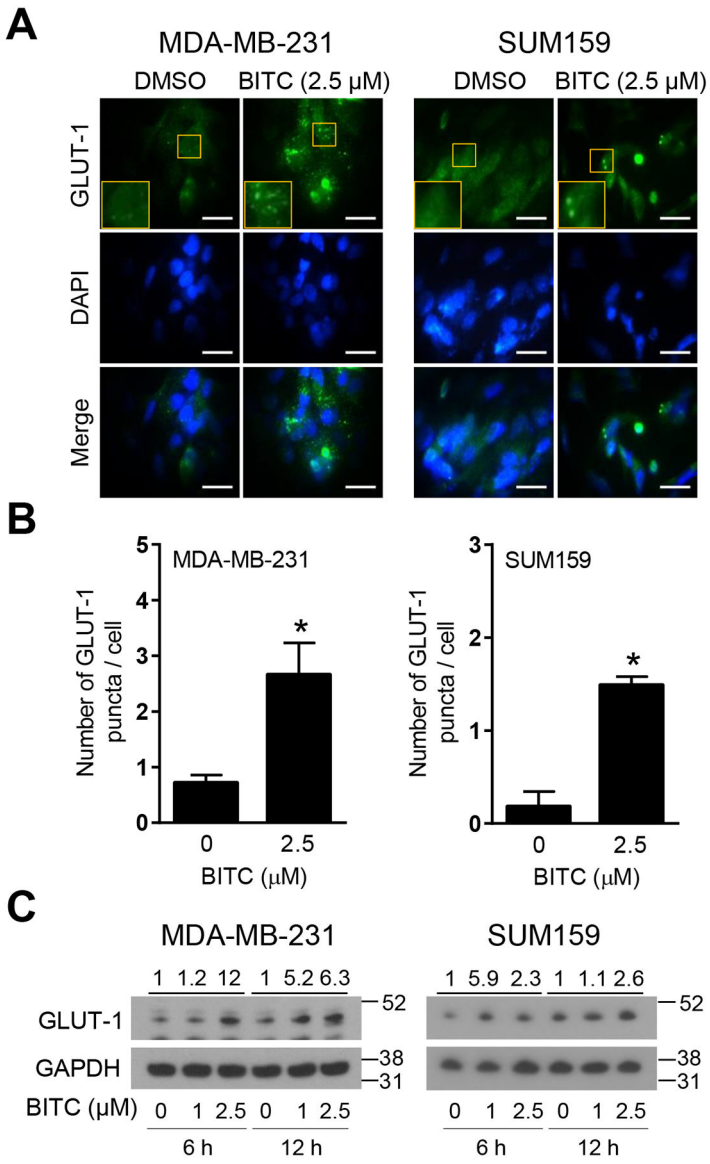

FIGURE 2.

Effect of BITC on translocation of GLUT-1 to the plasma membrane and changes in protein levels in human breast cancer cells. (A) Representative fluorescence microscopy images for GLUT-1 in MDA-MB-231 and SUM159 cells. The cells were treated for 24 h with DMSO (control) and 2.5 μM of BITC. Fluorescence microscopy images were taken at 100 × objective magnification (scale bar = 30 μm). Zoomed images of GLUT-1 puncta are shown in the yellow boxes. The staining for GLUT-1 is shown in green and for nuclei (DAPI) in blue. (B) Quantitation of number of GLUT-1 puncta per cell in MDA-MB-231 and SUM159 cell lines. Experiment was done twice with consistent results and representative data from one such experiment is shown as mean ± SD (n = 3). Statistical significance of differences (*, $P < 0.05$) was determined by unpaired Student *t* test. (C) Expression of GLUT-1 protein in MDA-MB-231 and SUM159 cells upon BITC (1 and 2.5 μM) treatment for 6 h and 12 h. Experiment was done at least twice and representative data from one such experiment are

shown. Numbers above bands are fold change in expression level of GLUT-1 relative to corresponding DMSO-treated control. Molecular size markers are added to the right side of blots.

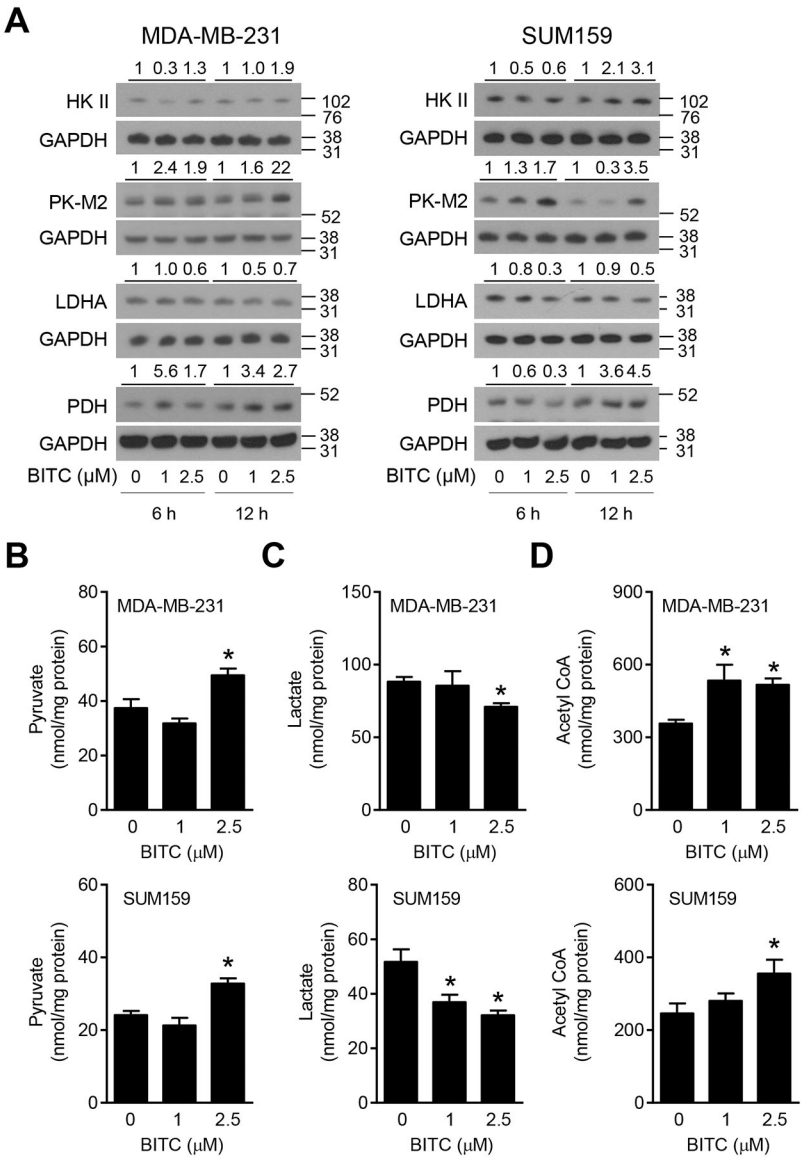

FIGURE 3.

Effect of BITC on glycolysis and TCA cycle proteins. (A) Western blotting for glycolysis and TCA cycle-related proteins in the lysates of DMSO (control)- or BITC (1 and 2.5 μM)-treated MDA-MB-231 and SUM159 cells (6 h and 12 h). Numbers above the blots indicate the fold change in protein level compared to corresponding DMSO-treated control. Molecular size markers are added to the right side of the blots. Experiments were done at least twice and representative blots from one such experiment are shown. Levels of intracellular pyruvate (B), secreted lactate (C), and intracellular acetyl CoA (D) in MDA-MB-231 and SUM159 cells treated for 24 h with DMSO (control) or BITC (1 and 2.5 μM). Experiments were done at least twice and representative data from one such experiment is shown as mean ± SD. Statistical significance of differences (*, $P < 0.05$) was determined by One-way ANOVA followed by Dunnett's test.

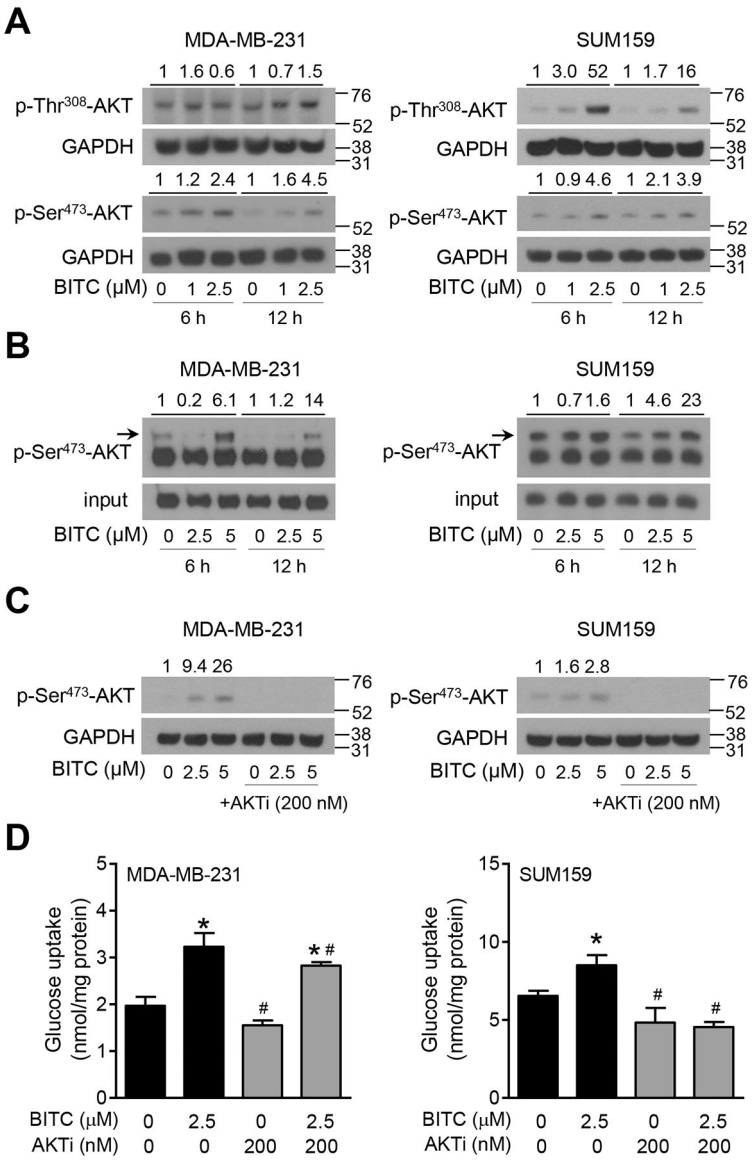

FIGURE 4.

Role of AKT in breast cancer metabolism after BITC treatment. (A) Immunoblotting for phospho-AKT Ser^{473} and Thr^{308} in MDA-MB-231 and SUM159 cells upon BITC (1 and 2.5 μM) treatment (6 h and 12 h). Numbers above the blots indicate the fold changes in protein levels compared to corresponding DMSO-treated control and molecular size markers are added to the right side of the blots. (B) AKT kinase activity in MDA-MB-231 and SUM159 cells upon BITC (2.5 and 5 μM) treatment for 6 h and 12 h. Experiments were done at least twice and representative data from one such experiment are shown. Numbers above the blots indicate the fold changes in protein levels compared to corresponding DMSO-treated control. (C) Immunoblotting for p-Ser^{473}-AKT in MDA-MB-231 and SUM159 cells treated with DMSO (control) or BITC (2.5 and 5 μM) with or without AKTi MK-2206 (200 nM) for 24 h. Numbers above the blots indicate the fold changes in protein levels compared to DMSO-treated control. (D) Quantitation of glucose uptake in MDA-MB-231 and SUM159

cells treated with DMSO (control) or BITC (2.5 μM) with or without AKTi MK-2206 (200 nM) for 24 h. Experiments were repeated at least twice (n = 3 for MDA-MB-231 and n = 4 for SUM159). Representative data from one such experiment is shown as mean ± SD. Statistically significant ($P < 0.05$) compared with the *corresponding DMSO-treated control or #between without AKTi MK-2206 and with AKTi MK-2206 by One-way ANOVA followed by Newman-Keuls multiple comparisons test.

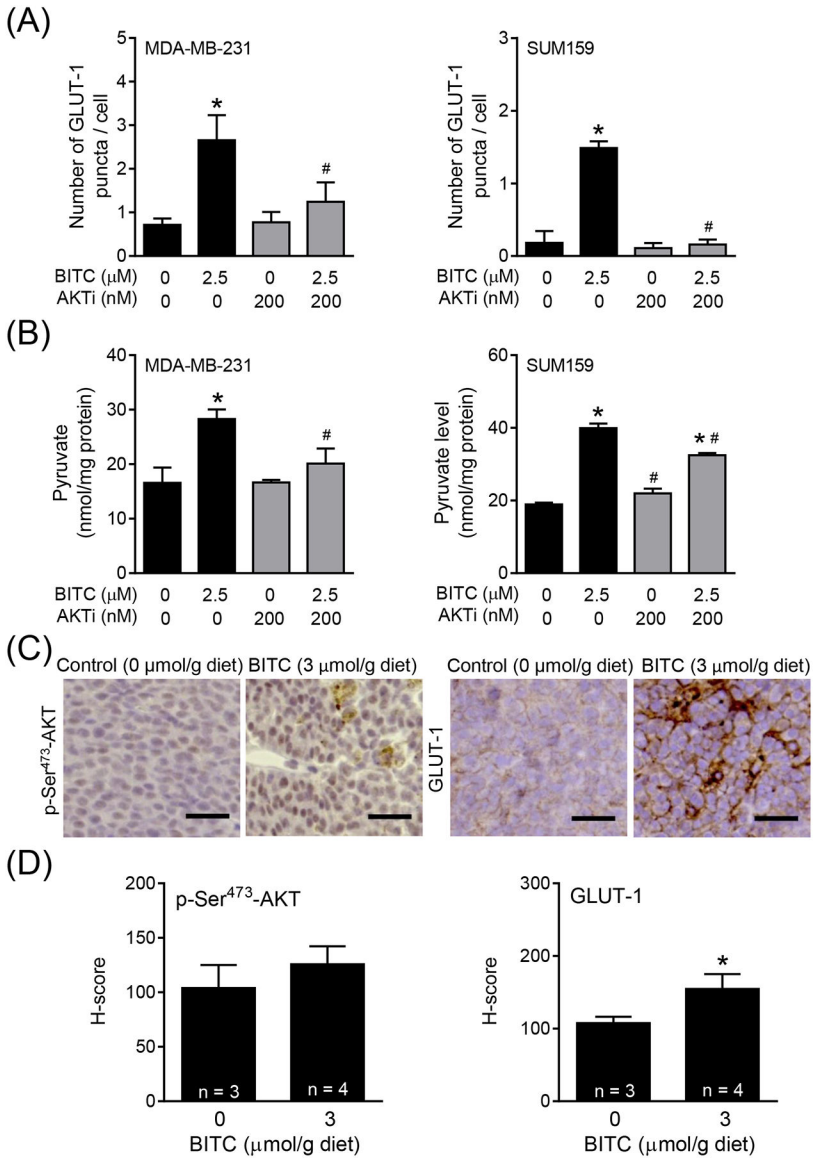

FIGURE 5.

Crosstalk between AKT and glucose metabolism in the presence of BITC. Quantitation of (A) GLUT-1 puncta per cell and (B) intracellular pyruvate level in MDA-MB-231 and SUM159 cells treated with DMSO (control) or BITC (2.5 μM) in combination with or without AKTi MK-2206 (200 nM) for 24 h. Experiment was repeated at least twice and representative data from one such experiment are shown as mean ± SD (n = 3). Statistically significant ($P < 0.05$) compared with the *corresponding DMSO-treated control or #between without AKTi (MK-2206) and with AKTi (MK-2206) by One-way ANOVA followed by Newman-Keuls multiple comparisons test. (C) Representative immunohistochemical images showing expression of p-Ser^{473}-AKT and GLUT-1 proteins in the tumor sections of control- or BITC-treated (3 μmol/g) mouse (200 × magnification; scale bar = 50 μm). (D) Quantitation of p-Ser^{473}-AKT and GLUT-1 shown in panel C. Immunohistochemical staining was analyzed by positive pixel algorithm for p-Ser^{473}-AKT and membranous

algorithm for GLUT-1 using Aperio ImageScope software (n = 3 from control and n = 4 from BITC-treated group). Statistical significance of differences (*, $P < 0.05$) was determined by two-sided unpaired Student *t* test.

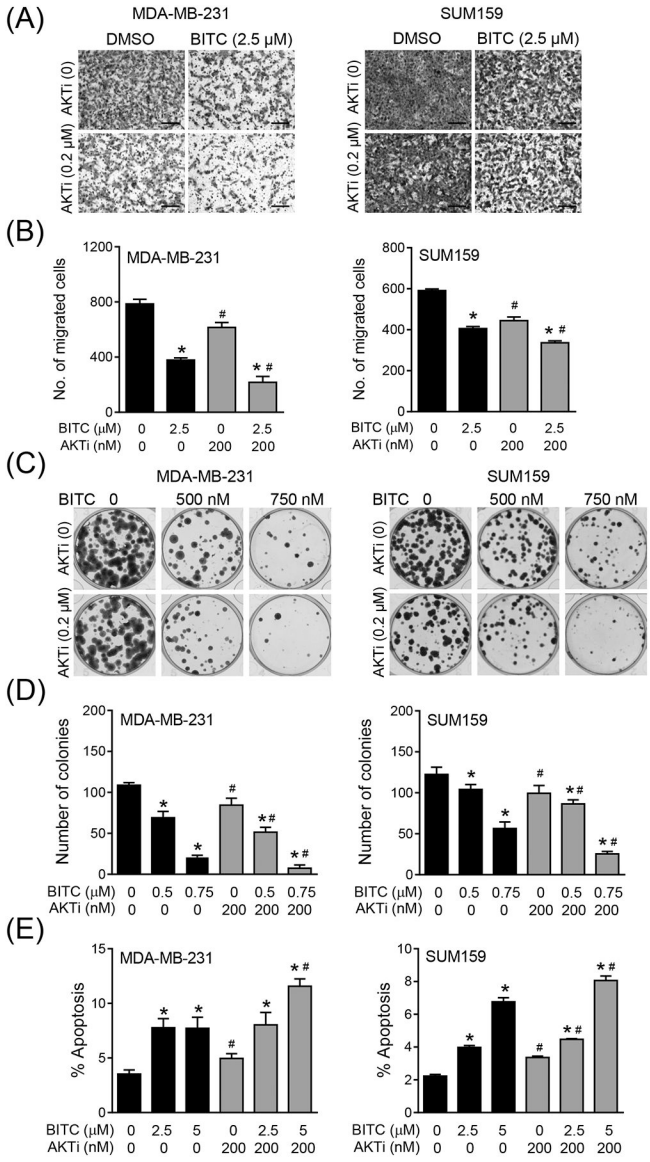

FIGURE 6.

Effect of AKT inhibition on migration, colony formation, and apoptosis in response to BITC treatment. (A) Migration in MDA-MB-231 and SUM159 cells upon treatment with DMSO (control) or 2.5 μM of BITC in combination with or without AKTi MK-2206 (200 nM) for 24 h. Representative images for migration are shown (200 × magnification; scale bar = 200 μm). (B) Quantitation of migration in MDA-MB-231 and SUM159 cells shown in panel A. Experiment was repeated at least twice and representative data from one such experiment are shown as mean ± SD (n = 3). Statistically significant ($P < 0.05$) compared with the *corresponding DMSO-treated control or #between without AKTi (MK-2206) and with AKTi (MK-2206) by One-way ANOVA followed by Newman-Keuls multiple comparisons test. (C) Colony formation in MDA-MB-231 and SUM159 cells after 10 days of treatment with DMSO (control) or indicated concentrations of BITC in combination with or without AKTi MK-2206 (200 nM). (D) Quantitation of colony formation shown in panel C.

Experiment was repeated at least twice and representative data from one such experiment are shown as mean ± SD (n = 3). Statistically significant ($P < 0.05$) compared with the *corresponding DMSO-treated control or #between without AKTi (MK-2206) and with AKTi (MK-2206) by One-way ANOVA followed by Newman-Keuls multiple comparisons test. (E) Apoptosis measured by Annexin V/PI in MDA-MB-231 and SUM159 cells upon treatment with DMSO (control) or BITC (2.5 and 5 μM) in combination with or without AKTi MK-2206 (200 nM). Each experiment was repeated at least twice and representative data from one such experiment are shown as mean ± SD (n = 3). Statistically significant ($P < 0.05$) compared with the *corresponding DMSO-treated control or $^{\#}$between without AKTi MK-2206 and with AKTi MK-2206 by One-way ANOVA followed by Newman-Keuls multiple comparisons test.